forests

MDPI

Article

Enhanced Isohydric Behavior Decoupled the Whole-Tree Sap Flux Response to Leaf Transpiration under Nitrogen Addition in a Subtropical Forest

Zhen Zhao [1], Ping Zhao [2], Zhenzhen Zhang [1,3,*], Lei Ouyang [2], Xiuhua Zhao [2], Liwei Zhu [2], Chenchen Cao [1] and Linhui Zeng [1]

[1] College of Geography and Environmental Sciences, Zhejiang Normal University, Jinhua 321004, China
[2] South China Botanical Garden, Chinese Academy of Sciences, Guangzhou 510650, China
[3] Key Laboratory of Watershed Earth Surface Processes and Ecological Security, Zhejiang Normal University, Jinhua 321004, China
* Correspondence: zhangzhen@zjnu.cn

Abstract: Anthropogenic nitrogen deposition has the potential to change the leaf water-use strategy in the subtropical region of China. Nevertheless, the whole-tree level response crucial for the ecosystem functions has not been well addressed over the past decades. In this study, the stem sap flux density (J_S) was monitored for the whole-tree water transport capacity in two dominant species (*Schima superba* and *Castanopsis chinensis*) in a subtropical forest. To simulate the increased nitrogen deposition, the NH_4NO_3 solutions were sprayed onto the forest canopy at 25 kg ha^{-1} year^{-1} (CAN25) and 50 kg ha^{-1} year^{-1} (CAN50), respectively, since April 2013. The J_S and microclimate (monitored since January 2014) derived from the whole-tree level stomatal conductance (G_S) were used to quantify the stomatal behavior (G_S sensitive to vapor pressure deficit, $G_{S\text{-}VPD}$) in response to the added nitrogen. The maximum shoot hydraulic conductance ($K_{shoot\text{-}max}$) was also measured for both species. After one-year of monitoring in January 2015, the mid-day ($J_{S\text{-}mid}$) and daily mean ($J_{S\text{-}mean}$) sap flux rates did not change under all the nitrogen addition treatments ($p > 0.05$). A consistent decline in the $G_{S\text{-}VPD}$ indicated an enhanced isohydric behavior for both species. In addition, the $G_{S\text{-}VPD}$ in the wet season was much lower than that in the dry season. *S. superba* had a lower $G_{S\text{-}VPD}$ and decreased $J_{S\text{-}mid}/J_{S\text{-}mean}$, implying a stronger stomatal control under the fertilization, which might be attributed to the low efficient diffuse-porous conduits and a higher J_S. In addition, the G_S for *S. superba* decreased and the $G_{S\text{-}VPD}$ increased more under CAN50 than that under CAN25, indicating that the high nitrogen dose restrains the extra nitrogen benefits. Our results indicated that the J_S for both species was decoupled from the leaf transpiration for both species due to an enhanced isohydric behavior, and a xylem anatomy difference and fertilization dose would affect the extent of this decoupling relation.

Keywords: canopy nitrogen addition; whole-tree water transport capacity; vapor pressure deficit; stomatal sensitivity; anatomical structure

check for updates

Citation: Zhao, Z.; Zhao, P.; Zhang, Z.; Ouyang, L.; Zhao, X.; Zhu, L.; Cao, C.; Zeng, L. Enhanced Isohydric Behavior Decoupled the Whole-Tree Sap Flux Response to Leaf Transpiration under Nitrogen Addition in a Subtropical Forest. *Forests* **2022**, *13*, 1847. https://doi.org/10.3390/f13111847

Academic Editor: Steven McNulty

Received: 30 September 2022
Accepted: 31 October 2022
Published: 4 November 2022

Publisher's Note: MDPI stays neutral with regard to jurisdictional claims in published maps and institutional affiliations.

Copyright: © 2022 by the authors. Licensee MDPI, Basel, Switzerland. This article is an open access article distributed under the terms and conditions of the Creative Commons Attribution (CC BY) license (https://creativecommons.org/licenses/by/4.0/).

1. Introduction

During the past decades, anthropogenic nitrogen (N) has been largely released into the atmosphere and deposited on terrestrial ecosystems in subtropical China [1–4]. Since N is critical for plant growth [5], the deposited N may affect the forest ecosystem functions such as the plant productivity and biodiversity [3,4,6,7], via changing their water use strategies [8–10].

Previous studies have showed that enhanced leaf hydraulic conductivity and transpiration rates were attributed to an extra N deposition via the leaf-level measurements [11–14]. Generally, the enhanced leaf transpiration increases the water potential gradient from the root to the leaf, driving the water flow in the plant stem within the SPAC (soil-plant-air

continuum) systems [15–18]. However, leaf transpiration cannot be always maintained, and it would decrease when excessive water consumption occurs (for example, during the noon in a shiny day) to maintain above a threshold leaf water potential, i.e., the isohydric behavior [19,20]. In other words, the benefits of an increased N addition on the leaf transpiration would be neutralized if the water transport capacity of the stem did not meet the increased transpiration demands [21,22]. However, few studies have been conducted to validate this hypothesis.

It is noted that the isohydric behavior is not necessarily adopted by all species. Some species have the ability to maintain a high leaf transpiration even under a low water potential (anisohydric behavior) in order to optimize the carbon allocation [23,24]. Previous studies suggested that the xylem conduits' characteristics differences will influence the stomatal behavior [20,23]. The ring-porous species with large conduits (higher transient water transport capacity) generally tend to be anisohydric, whereas the diffuse-porous species with small conduits tend to be isohydric [16,25]. Thus, we speculated that the consistent increase in the leaf and whole-tree water transports would occur for the ring-porous species, not for the diffuse-porous species.

In addition, studies indicated that the isohydric–anisohydric behavior may not be maintained across the whole year [26,27]. Some plants could switch their isohydric-like behavior in the wet season to anisohydric-like behavior in response to the drought conditions [28,29]. This behavior was considered as a trade-off between hydraulic safety and carbon assimilation [26]. Since a nitrogen addition could increase the leaf transpiration [29], it was expected that the switch of the anisohydric–isohydric could be enhanced due to a N input for the anisohydric species, and the isohydric behavior for the isohydric species could be enhanced in drought conditions. In subtropical China, wet and dry seasons are divided according to their distinct precipitation regime [30]. Thus, plants would behave more isohydrically in the dry season. We expected that this anisohydric–isohydric switch could be regulated by the nitrogen addition in this region.

In this study, two evergreen species (*Schima superba* Gardn. et Champ. and *Castanopsis chinensis* Hance) in our plots were selected to conduct fertilization experiments; these species have the highest importance value, implying their dominated role in the forest community [14]. They were also categorized into the diffuse-porous and ring-porous species, respectively [31]. A canopy fertilization was performed to simulate the natural N deposition [14]. The sap flux was monitored for whole-tree water transport capacity. The aim was to test:

1. Whether the whole-tree water transport capacity would consistently be enhanced by the N additions;
2. Whether the above behavior would be impacted by the xylem anatomy differences between the two species and wet–dry season switch.

2. Materials and Methods

2.1. Site and Treatment Description

The experiment was conducted in the Shimentai National Nature Reserve in Northern Guangdong Province, China (24°22′–24°31′ N, 113°05′–113°31′ E, Figure 1A). This region was characterized by a low subtropical monsoon climate, with an average annual temperature of 19 °C and a precipitation of 1800 mm. Most of the precipitation falls in the wet season (from April to September) [14]. The vegetation is typically dominated by low subtropical evergreen broad-leaf forests. The forest canopy height was around 16 m. The N deposition in this region was reported as 21.5 kg N ha^{-1} $year^{-1}$ in 2013 [32], and this value should double by 2050 [33].

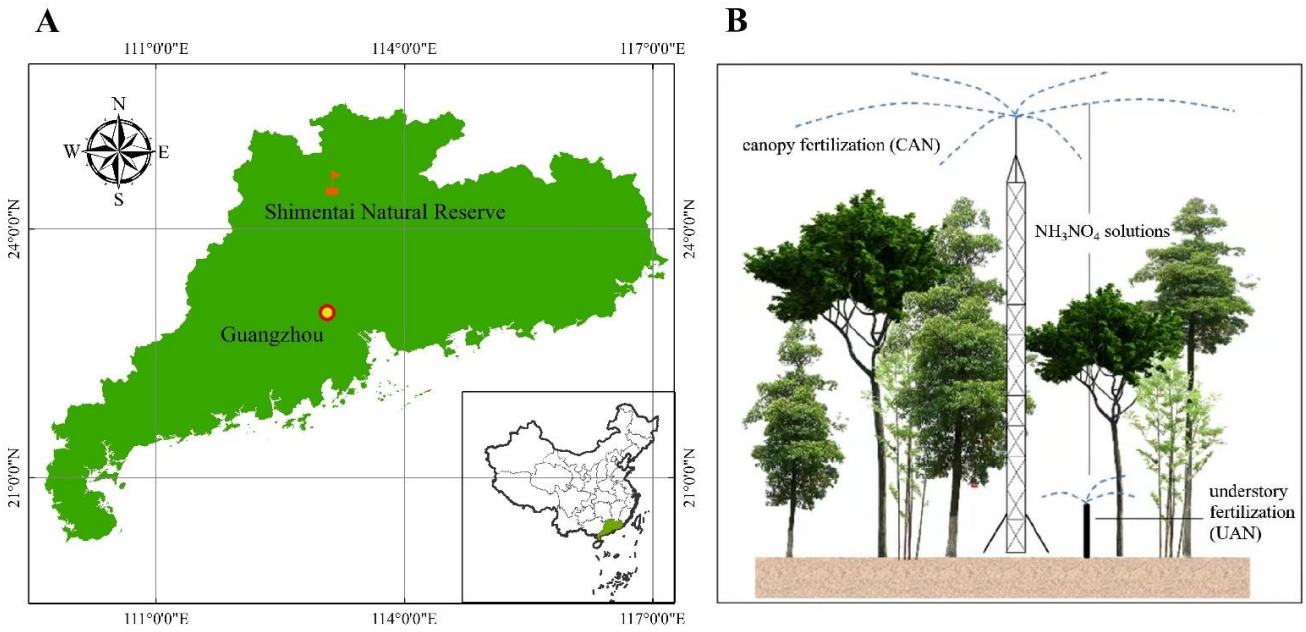

Figure 1. Location of the study site (**A**) and diagram of the simulated N addition (**B**).

In this study, the N addition treatments were conducted from the canopy (CAN) of the forest with an iron tower (35 m) (Figure 1B). The following treatments were designed: the control (CK, without N addition); CAN25 (25 kg N ha^{-1} $year^{-1}$); and CAN50 (50 kg N ha^{-1} $year^{-1}$) to simulate a double (CAN25) and triple (CAN50) N deposition compared to a background wet deposition (CK). In addition, the traditional understory fertilization was also monitored in other plots that were independent of CK and CAN. All these plots were arranged by a randomized blocks design with a >50 m gap among different plots to avoid their interactions. However, this was not considered in our study (Figure 1B). Three 20 m × 20 m plots were designed for each treatment. The NH_4NO_3 solutions were sprayed over the canopy from the iron tower (35 m) (Figure 1B). The treatments started from April to October (the growing season) in 2014 (7 times a year). According to Zhang et al. [34], over 95% of the solutions were evenly sprayed with each plot. More details of this experiment can be found in Zhang et al. [14].

2.2. Sap Flux and Stomatal Conductance

The sap flux density (J_S, g m^{-2} s^{-1}) was measured on 38 (4–5 individuals in each plot) *S. superba* and 60 *C. chinensis* (5–6 individuals in each plot) individuals by self-made TDPs (thermal dissipation probes) sensors [35] from January to December 2014. After the probes malfunction (especially in the wet season, almost once every 2 months for one individual), the same probes will be used as a substitution. All these individuals had a DBH > 10 cm, i.e., they were adults. The sapwood depth ranged 4~15 cm and 6~13 cm, respectively, for *S. superba* and *C. chinensis*, respectively. The sensors consisted of a pair of 2 cm long probes in aluminum tubes, which were inserted 15 cm apart into the trunk at the breast height (1.3 m above ground). The upper probes were constantly heated at 0.2 W to produce thermal differences with the lower probes (ΔT). All sensors were wrapped in a plastic cover and aluminum foil to prevent the disturbance of mechanical damage, rain soaking, and solar radiation. The J_S was calculated by ΔT according to the empirical formula [35]:

$$J_S = a \times [(\Delta T_{max} - \Delta T)/\Delta T]^b \quad (1)$$

where ΔT_{max} was the ΔT under zero flux conditions. A night-time leaf stomatal conductance in three typical sunny days was tested in both dry and wet seasons, confirming the zero transpiration at the mid-night. ΔT was converted into a voltage value and was recorded with a data logger (DL2e, Delta-T Devices, UK) every 10 min. a and b are the empirical

coefficient for a specific species. In order to determine the coefficient of the two species, a validation experiment was conducted. Three stem segments for each species were fixed upside down on a supporting stand, and purified water was designed to flow downward through the stem. A container was placed on a balance underneath the segment to collect and record the water flowing through the segment (J_k). The sap flux inserted on the stem was synchronously measured by TDPs. The a and b were derived from the dataset of J_k and ΔT based on Equation (1) (the specific methods were included in Zhang et al. [18]). The a and b for *S. superba* and *C. chinensis* were 106, 0.989 and 154, 1.146, respectively.

Since a system malfunction usually occurred every week for some probes due to lightning, an insect bite, a short circuit, etc., the data gap needed to be filled before conducting the analysis. The monitored data before the malfunction was fitted to that of the most closed trees. The fitting functions were then used to predict the lost data.

According to Köstner et al. [36], a stomatal conductance (G_S) of the canopy can be estimated based on a simplified equation:

$$G_S = (G_V T_a \rho E_L)/VPD \quad (2)$$

where G_V is the universal gas constant adjusted for the water vapor (0.462 m^3 kPa K^{-1} kg^{-1}), T_a is the air temperature (°C), ρ is the density of water (998 kg m^{-3}), and VPD is the vapor pressure deficit calculated by the T_a and relative humidity (RH, %) [37]. The E_L is whole-tree transpiration per unit leaf area calculated by the sapwood area (A_S) and the total leaf area (A_L). The A_S and A_L were calculated based on the allometric relationship with the stem diameter at the breast height (DBH), which was detailed in our previous study [38]. There is no significant difference in the leaf area index, tree height, and DBH for both species before and after our experiment, which lasted for one year (Figure S2).

2.3. Shoot Hydraulic Conductance

The shoot hydraulic conductance was measured using HPFM (HPFM Gen3; Dynamax Corp., Elkhart, IN, USA) under a quasi-steady-state mode. After finishing the sap flux measurements, 15 shoots were cut from the sunlit canopy under each treatment for the two species. These shoots were soaked and wrapped and immediately moved to the lab. They were perfused with the KCl solution at a pressure of ~0.5 MPa until a stable flow rate was reached. All the leaflets were then cut off and the hydraulic conductance of the shoot without leaves was measured. The environmental temperature was automatically recorded by the HPFM and all the conductance measurements were corrected to values at 25 °C.

2.4. Environmental Factors

A micro-meteorological station was established in an open field with an area of 50 m^2 surrounding our sites to represent the forest canopy environmental conditions. Photosynthetically active radiation (PAR, mol m^{-2} s^{-1}, SKP 215, London, UK), T_a, RH (Model AV-S3 Temperature and Relative Humidity Probe), and wind speed (v, m s^{-1}, SM300, London, UK) were measured simultaneously with the sap flux measurements.

2.5. Data Analysis

To characterize the water use strategy, the daily mean J_S and G_S (6:00–18:00) ($J_{S\text{-mean}}$ and $G_{S\text{-mean}}$) were calculated, excluding the nocturnal data. In addition, the mid-day data (11:00–13:00) was also derived to depict the maximum water transport potential ($J_{S\text{-mid}}$ and $G_{S\text{-mid}}$) for each tree individual. Considering the dry/wet oscillation throughout the year, those data were divided into dry and wet seasons.

A boundary line analysis was adopted to depict the essential relation between the VPD and G_S [39]. The specific progress of the boundary line analysis was depicted in Zhang et al. [40]. To define the stomatal sensitivity to VPD, the boundary line data of the G_S was log-transformed and linearly fitted to the VPD (Figure S1), and the slopes ($G_{S\text{-VPD}}$) were used to characterize the stomatal controlling sensitivity to canopy the water loss, i.e., the isohydric behavior. The decreased $G_{S\text{-VPD}}$ under the fertilization treatments implied an

enhanced stomatal control (a behavior more likely isohydric) and vice versa (a behavior more likely anisohydric).

An analysis of variance (ANOVA) was conducted with SPSS Statistics (v18.0, IBM Inc., Chicago, IL, USA) to evaluate the N fertilization treatment, seasonal change, and species difference effects (defined as Treatments, Seasons, and Species) on the J_S, G_S. $G_{S\text{-}VPD}$ was compared by an analysis of covariance (ANCOVA). All the data passed the normal distribution test. Origin pro (version 2019b, Origin Lab, Northampton, MA, USA) was used to draw the graphs.

3. Results

3.1. Effects of Fertilization on the Shoot Hydraulic Conductance

In our study, the *S. superba* and *C. chinensis* were typically diffuse-porous and ring-porous species, respectively, and the latter had a higher $K_{shoot\text{-}max}$ (Figure 2) than the former. However, all the nitrogen addition treatments did not change their $K_{shoot\text{-}max}$. These results indicated that the fertilization did not change the shoot water transport capacity for both species, even though they had a different xylem anatomy.

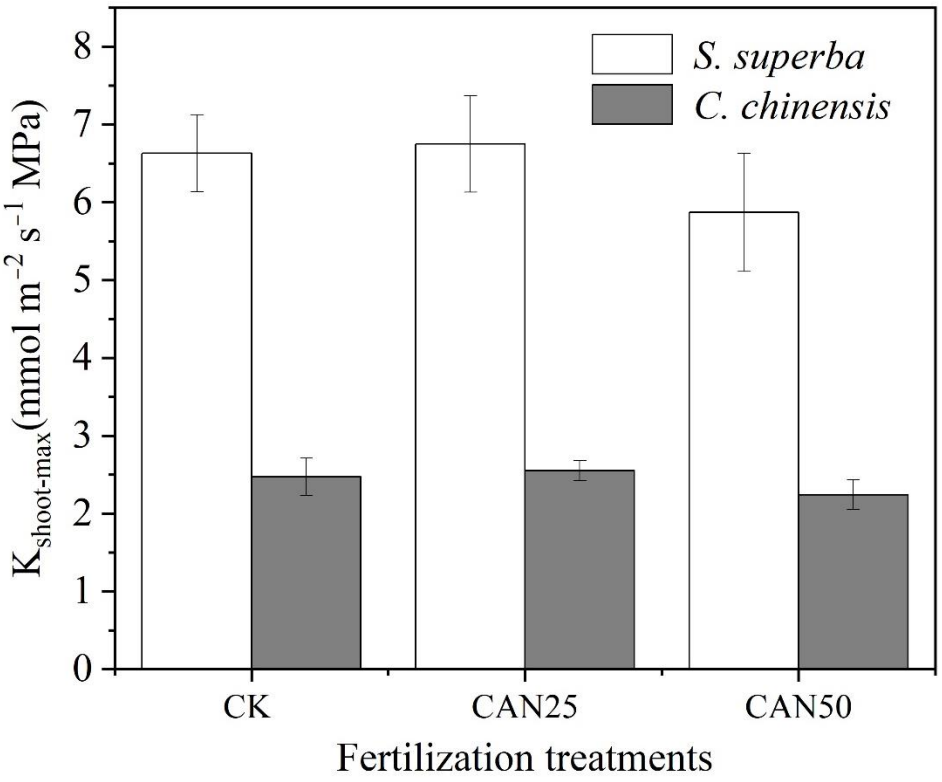

Figure 2. Comparison of the maximum shoot hydraulic conductance ($K_{shoot\text{-}max}$) among different fertilization treatments.

3.2. Sap Flux and Canopy Stomatal Conductance

The ANOVA indicated that all the three factors (seasons, species, and treatments) had an influence on the J_S. However, the interaction effects between the different factors were not observed (Table 1). The fertilization effects on the J_S were not significant for both the $J_{S\text{-}mid}$ and $J_{S\text{-}mean}$ (Figure 3). Comparably, both of the $J_{S\text{-}mid}$ and $J_{S\text{-}mean}$ were significantly influenced by the wet–dry season oscillation. The $J_{S\text{-}mid}$ and $J_{S\text{-}mean}$ in the wet season (19.59 and 13.09 g m^{-2} s^{-1}) were obviously higher than that in the dry season (11.60 and 7.12 g m^{-2} s^{-1}) ($p < 0.01$, Figure 3). Among the different species, *S. superba* had a higher $J_{S\text{-}mid}$ (17.86 g m^{-2} s^{-1}) and $J_{S\text{-}mean}$ (11.66 g m^{-2} s^{-1}) than *C. chinensis* (12.65 and 7.90 g m^{-2} s^{-1}) ($p < 0.01$, Figure 3).

Table 1. ANOVA on the $J_{S\text{-}mean}$ and $J_{S\text{-}mid}$.

Source	$J_{S\text{-}mean}$			$J_{S\text{-}mid}$		
	df	F	Sig	df	F	Sig
Corrected Model	19	5.880	0.000	19	6.084	0.000
Seasons	1	92.770	0.000	1	75.986	0.000
Species	1	17.353	0.000	1	15.008	0.000
Treatments	4	6.146	0.000	4	5.530	0.000
Seasons × Treatments	4	1.216	0.304	4	1.330	0.258
Species × Treatments	4	1.800	0.129	4	1.529	0.193
Seasons × Species	1	0.036	0.849	1	0.037	0.847
Seasons × Species × Treatments	4	1.823	0.124	4	1.959	0.100

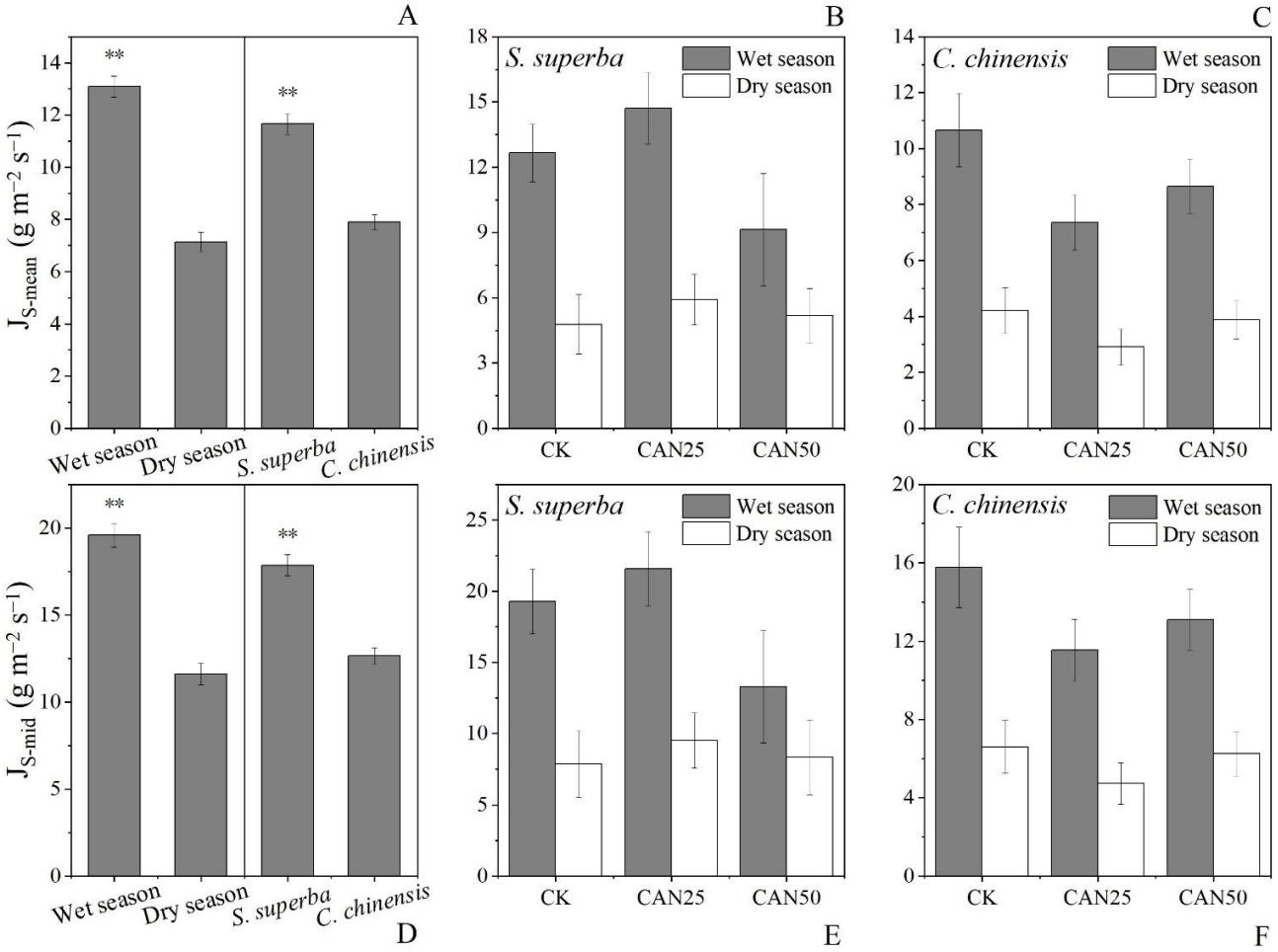

Figure 3. Daily mean J_S ($J_{S\text{-}mean}$) and mid-day J_S ($J_{S\text{-}mid}$) under different seasons and speciesv (**A**,**D**), $J_{S\text{-}mean}$ and $J_{S\text{-}mid}$ of *S. superba* and *C. chinensis* under nitrogen addition treatments (**B**,**C**,**E**,**F**). The error bars indicate the standard error. ** indicate significant differences at $p < 0.01$.

The ANOVA showed that $G_{S\text{-}mid}$ and $G_{S\text{-}mean}$ were affected by the species and treatments, but not seasons (Table 2). Meanwhile, both seasons and species had interactions with the treatments (Table 2). *S. superba* had a higher $G_{S\text{-}mean}$ and $G_{S\text{-}mid}$ than *C. chinensis* (Figure 4). The $G_{S\text{-}mean}$ and $G_{S\text{-}mid}$ for *S. superba* increased significantly under all the treatments. Individuals under a lower fertilization dose (25 kg ha^{-1} year^{-1}) had a higher $G_{S\text{-}mean}$ and $G_{S\text{-}mid}$ increase than that under a higher dose (50 kg ha^{-1} year^{-1}) in the wet and dry seasons. However, similar patterns were not observed for *C. chinensis* (Figure 4), and there was no apparent change in the $G_{S\text{-}mean}$ and $G_{S\text{-}mid}$ in both dry and wet seasons (Figure 4).

Table 2. ANOVA on the $G_{S\text{-}mean}$ and $G_{S\text{-}mid}$.

Source	$G_{S\text{-}mean}$			$G_{S\text{-}mid}$		
	df	F	Sig	df	F	Sig
Corrected Model	19	4.733	0.000	19	5.169	0.000
Seasons	1	1.582	0.209	1	0.235	0.628
Species	1	92.029	0.000	1	92.749	0.000
Treatments	4	6.923	0.000	4	6.821	0.000
Seasons × Treatments	4	2.599	0.036	4	3.127	0.015
Species × Treatments	4	4.943	0.001	4	3.995	0.004
Seasons × Species	1	0.051	0.822	1	0.358	0.550
Seasons × Species × Treatments	4	1.742	0.140	4	1.838	0.121

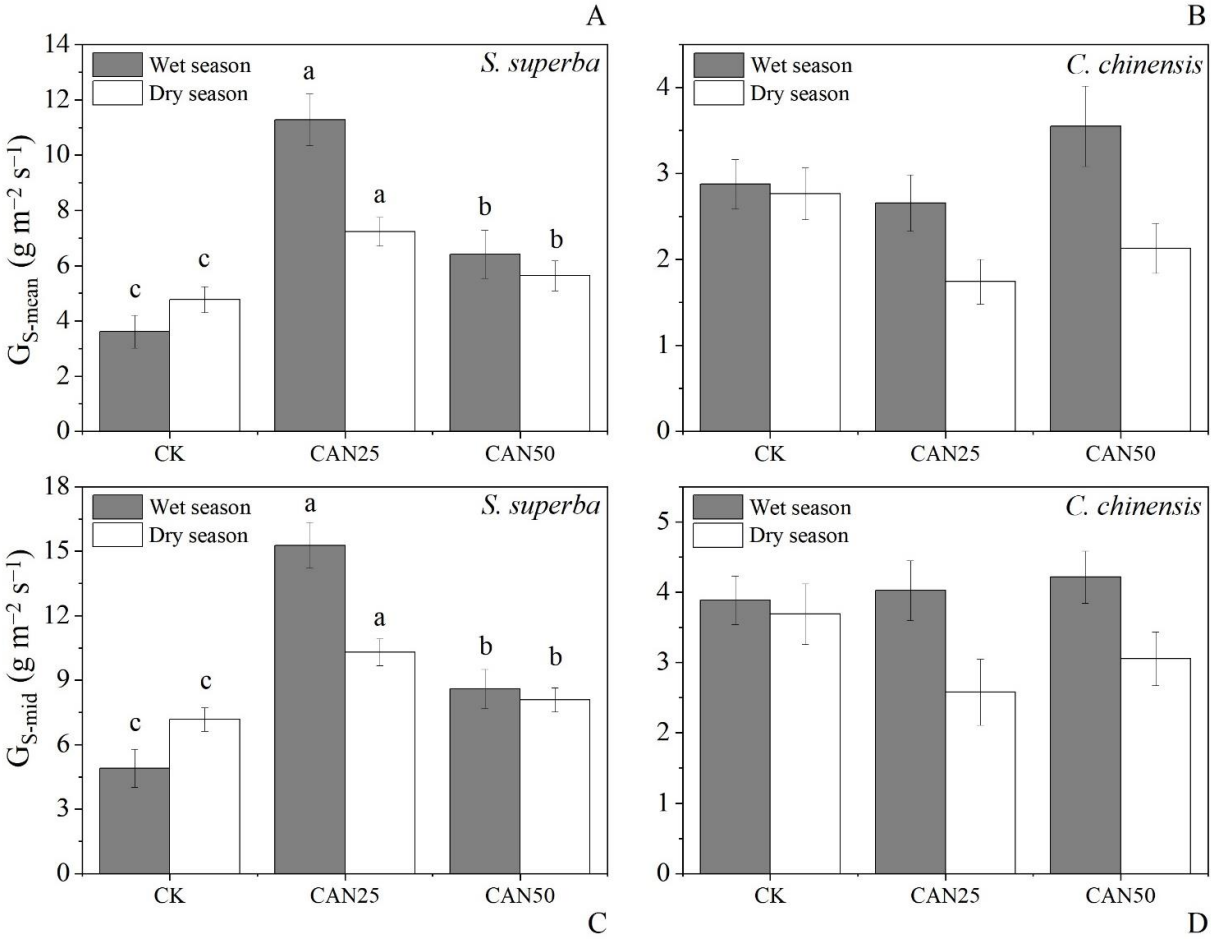

Figure 4. Daily mean stomatal conductance ($G_{S\text{-}mean}$) and mid-day stomatal conductance ($G_{S\text{-}mid}$) under different N treatments for *S. superba* (**A**,**C**) and *C. chinensis* (**B**,**D**), and in the dry and wet seasons, different letters indicate significant differences at $p < 0.05$.

In order to evaluate the canopy water stress intensity at noon under different treatments, the $J_{S\text{-}mid}$ was fitted to the $J_{S\text{-}mean}$ and the $G_{S\text{-}mid}$ was fitted to the $G_{S\text{-}mean}$ (Figure 5). The results showed that the slopes increased under all the N addition treatments for *S. superba* ($p < 0.05$); similar results were not observed for *C. chinensis*, and there was no significant influence of the nitrogen effects on the slopes (Figure 5). These results implied that a significant water stress occurred for *S. superba* due to the nitrogen input, but not for *C. chinensis*.

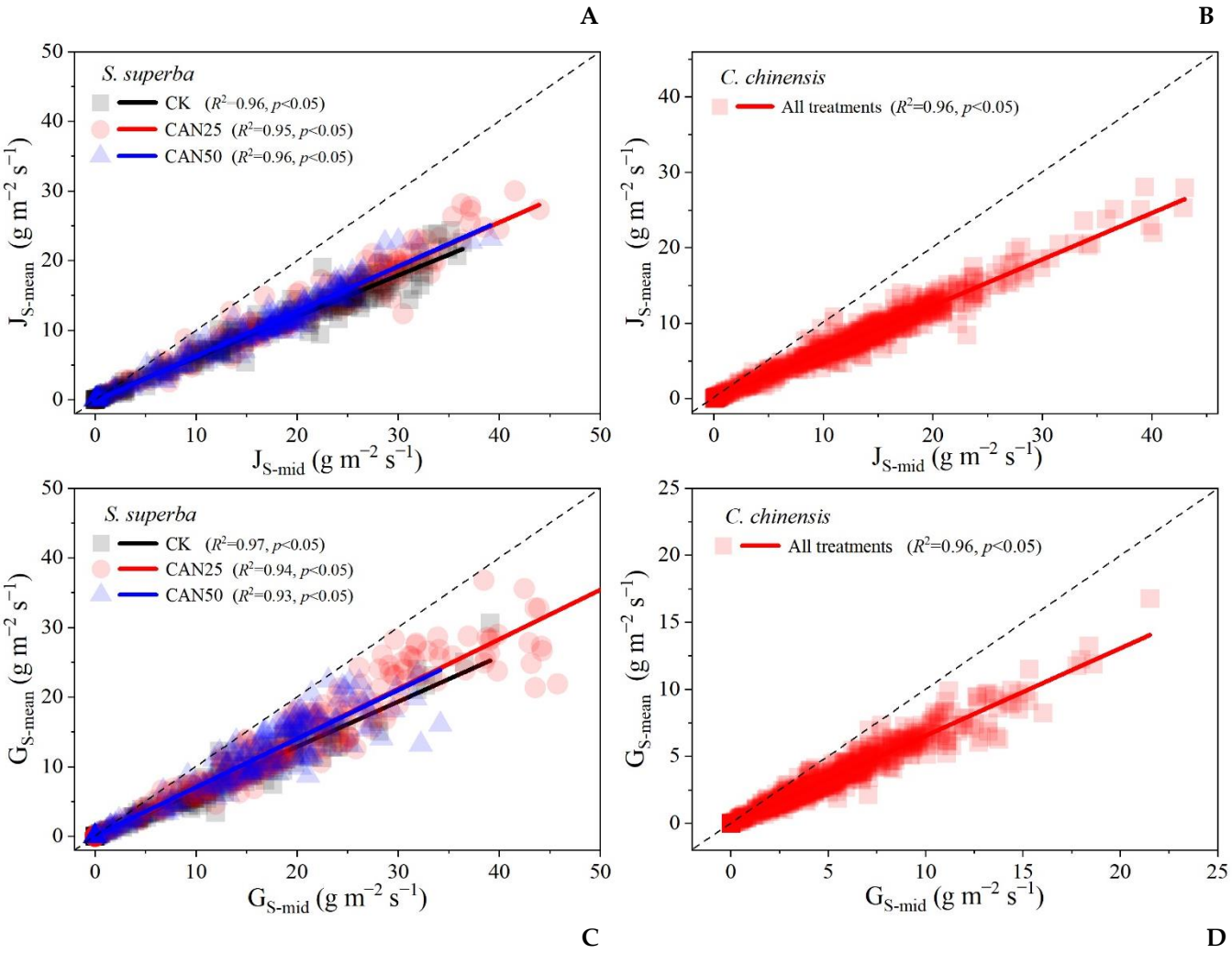

Figure 5. The mid-day J_S ($J_{S\text{-mid}}$) fitted daily mean J_S ($J_{S\text{-mean}}$) and the mid-day G_S ($G_{S\text{-mid}}$) fitted daily mean G_S ($G_{S\text{-mean}}$) for *S. superba* (**A**,**C**) and *C. chinensis* (**B**,**D**) under different nitrogen addition treatments. ANCOVA indicated that the differences of slopes under five nitrogen addition treatments were only significant for *S. superba*.

3.3. Stomatal Sensitivity

All the three factors including the seasons, species, and treatments had effects on the $G_{S\text{-VPD}}$ (Table 3). $G_{S\text{-VPD}}$ in the wet season was more negative than that in the dry season, and *S. superba* had a more negative $G_{S\text{-VPD}}$ than *C. chinensis* (Figure 6A). The $G_{S\text{-VPD}}$ significantly decreased under CAN25, indicating an enhanced stomatal control (Figure 6). This decline was not observed under the CAN50. Differences in the seasons and species did not interrupt the effect of the nitrogen (Table 3). The wet season had a more negative $G_{S\text{-VPD}}$ (−12.83) than the dry season ($p < 0.05$). *S. superba* had a more negative $G_{S\text{-VPD}}$ than *C. chinensis* ($p < 0.01$).

Table 3. Results of ANOVA for the G_S in response to VPD.

Source	df	F	Sig
Corrected Model	19	2.138	0.001
Seasons	1	8.765	0.004
Species	1	4.657	0.002
Treatments	4	6.243	0.014
Seasons × Treatments	4	0.540	0.707
Species × Treatments	4	2.429	0.051
Seasons × Species	1	0.183	0.670
Seasons × Species × Treatments	4	0.566	0.688

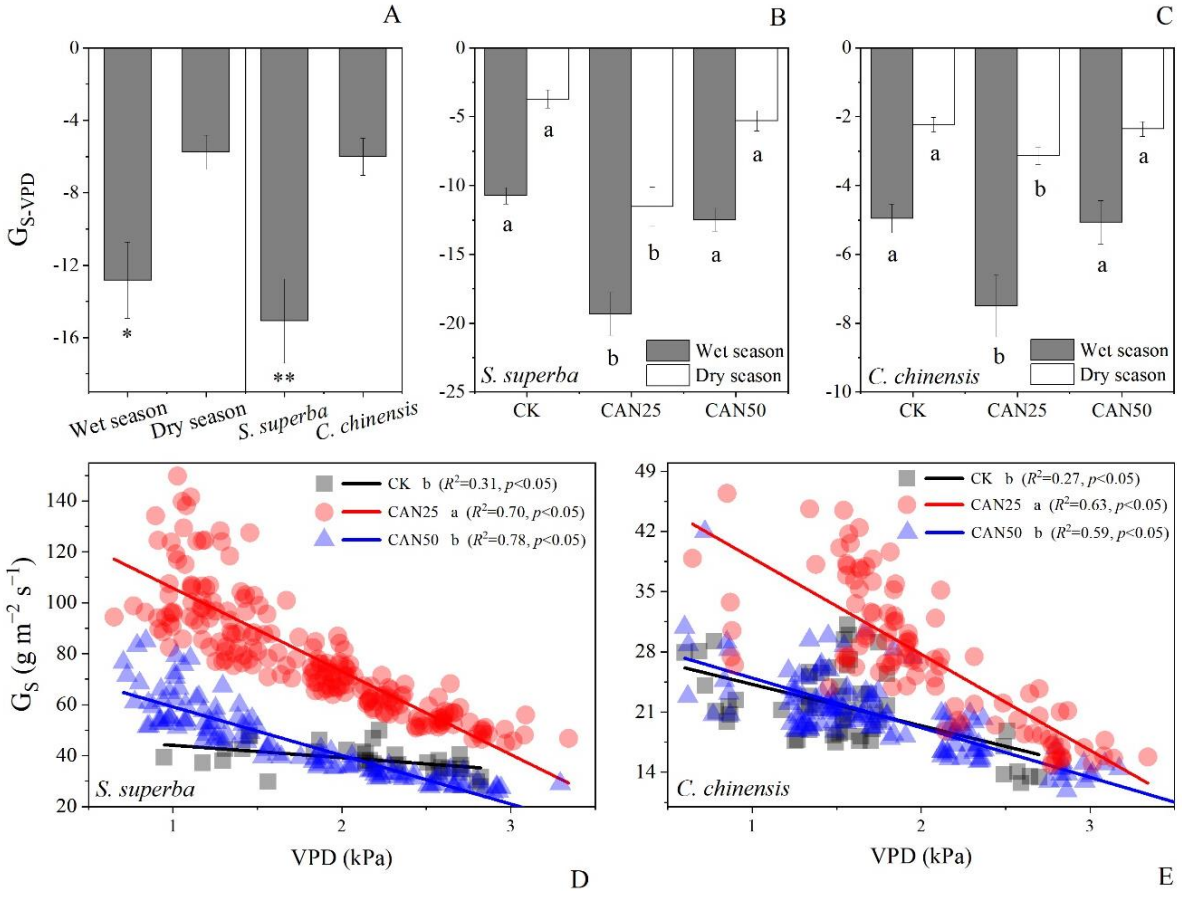

Figure 6. The mean values (**A**–**C**) and the linear fitting (**D**,**E**) of the slopes of VPD to G_S ($G_{S\text{-}VPD}$) under different nitrogen addition treatments (CK, CAN25, CAN50), in the dry and wet seasons, *S. superba* and *C. chinensis*, different letters indicate significant differences at $p < 0.05$; * indicate significant differences at $p < 0.05$; ** indicate significant differences at $p < 0.01$.

4. Discussion

4.1. Nitrogen Deposition on the Whole-Tree Water Transport Capacity

In this study, a weak fertilization effect on the whole-tree water transport capacity for both *S. superba* and *C. chinensis* was presented (Figure 3). Generally, the extra N input enhanced photosynthesis, which further increased the leaf water loss rates. Evidence was presented by the increased leaf N content, photosynthesis, and transpiration rates at the leaf scale [13,14]. While from the whole-tree aspect, weak variations of $J_{S\text{-}mid}$ and $J_{S\text{-}mean}$ under CAN25 and CAN50 were observed for both species (Figure 3), i.e., the whole-tree water transport capacity response was decoupled to that of the enhanced leaf transpiration reported in a previous study on these individuals [14].

The disagreement should be rooted in the decoupled hydraulic development of shoots and leaf hydraulic tissues. As argued, the enhanced leaf transpiration rate was attributed to the improved maximum leaf hydraulic conductance ($K_{leaf\text{-}max}$) [13], which could be validated by the enhanced canopy G_S under CAN25 (Figure 4). However, the leaf mesophyll resistance was not the only barrier of water transport within the SPAC. When the root and shoot resistance to the water transport were not released, and an excessive leaf water consumption could not be supplied timely, the leaf water potential would dramatically decrease [25]. In our study, the difference in the maximum shoot hydraulic conductance $K_{shoot\text{-}max}$ for *S. superba* and *C. chinensis* was not significant among the different treatments ($p < 0.01$, Figure 2). In another study, a weak effect on the xylem development was observed for all species after a two-year fertilization in our plot [41]. In other words, the shoot development under an extra N input was much slower than that of the leaf tissues. This out-of-step growth might not be necessarily relieved in the long run [42], since 6-year fertilization also did not show obvious fertilization effects on the cell production of mature black spruce [43].

It is noted that even though the leaf transpiration increased [14], the mid-day water potential was still maintained for both species [13], revealing the existence of the compensation system to prevent the continually decreased water potential. The isohydric behavior was usually initialized after the depletion of the water storage to maintain the minimum leaf water potential [20,44]. In our study, the isohydric behavior was even strengthened since the $G_{S\text{-}VPD}$ increased under CAN25 for both species (Figure 6, Table 3). Evidence could also be found in the consistently increased leaf P_{50} (reduced leaf hydraulic safety margin) for both species [13]. In addition, the above strengthened isohydric behavior had no interaction with the wet–dry switch (Table 3), i.e., the isohydric behavior was consistently enhanced in the wet and dry seasons.

To our surprise, a stronger stomatal control (lower $G_{S\text{-}VPD}$) was found in the wet season rather than in the dry season (Figure 6A), implying that the reduced water supply was not enough to induce a stomatal control. In another study, transpiration was even increased dramatically in a simulated experiment of reduced precipitations in this region [45]. The water isotope indicated the dominant trees in this region mostly use the deep soil water, especially in the dry season due to their deep roots [14,46]. The lower $G_{S\text{-}VPD}$ in the wet season could be attributed to the higher J_S (Figure 3) since the rainy season was also the growing season in our site [47]. Thus, the canopy transpiration demands might be crucial for the isohydric behavior shift [48].

4.2. Species Differences of the Nitrogen Effects

Even though the J_S for both species (*S. Superba* and *C. chinensis*) was maintained due to their stomatal control, *S. Superba* tended to behave more isohydrically, considering their $G_{S\text{-}VPD}$ was higher than *C. chinensis* (Figure 6A). Evidence was also provided by the reduced $J_{S\text{-}peak}/J_{S\text{-}mean}$ ratio, revealing the stronger water stress during the noon when the VPD was peaked (Figure 5). In addition, a similarly depressed leaf g_s was also observed only in the *S. superba* individuals under full light conditions in another study [14]. Accompanied with the intensified stomatal control, some structural acclimations such as a decreased leaf SLA and ^{13}C isotope abundance (implying increased water use efficiency) were also observed for *S. superba* in our previous study [14].

A xylem anatomy difference between *S. superba* and *C. chinensis* might account for their different responses. *S. superba* was characterized with higher J_S and G_S (Figures 3 and 4), which benefited from its higher water transport capacity provided by the small but numerous diffuse-porous conduits [31]. However, the price of the diffuse-porous conduits was a lower hydraulic efficiency [49]. *C. chinensis* had ring-porous conduits characterized by a higher water transport efficiency, thus responding to the leaf transpiration demands rapidly [49]. The water transport efficiency of one single conduit for *C. chinensis* and *S. superba* was reported as 1.31×10^{-5} kg·m·MPa^{-1}·s^{-1} and 2.26×10^{-8} kg·m·MPa^{-1}·s^{-1}, respectively [31]. A similar difference was also observed in the boreal forests, i.e., species

with large conduits experienced a weaker stomatal control [15,16]. Due to the slower water transport efficiency of small conduits for *S. superba*, the rapid depletion of the canopy water storage could not be replenished, leading to a stronger stomatal control than *C. chinensis* [23]. This behavior is likely to damage the carbon gain in the long run [50]. However, since only two species were investigated in our study, whether this pattern was universal for all the diffuse-porous species was uncertain.

4.3. Influence of the Fertilization Dose on the Nitrogen Effects

It was noted that the N addition effects on the stomatal control for *S. superba* were weakened and even offset under a high fertilization dose (Figure 6). Meanwhile, the largely enhanced G_S under CAN25 was counteracted by a high fertilization (Figure 4). Similar suppressed leaf-level gas changes under CAN50 were also observed at the leaf scale for these individuals in another study [14]. In addition, the J_S also tended to decrease, though not significantly (Figure 3). These results indicated that a high nitrogen restrain occurred on both the whole-tree and the leaf scale. In a study on Cassava (*Manihot esculenta* Crantz), a restrained transpiration, reduced photosynthesis, and decreased carbohydrate occurred when the N reached 200 mg N L^{-1}, finally leading to lower yields [51].

Some theories were proposed to explain these depressions [51]. Firstly, a high N input led to a rapid water loss, which stimulated a massive stomatal closure [51]. Thus, the variation of VPD tended to be less effective to the stomatal control [52,53], i.e., higher $G_{S\text{-}VPD}$ in our study (Figure 6). In addition, the carbon allocation strategy should also be responsible [54–56]. A meta-analysis on 54 studies found that nitrogen deposition resulted in a significantly decreased fine root biomass (<2 mm diameter; −12.8%) and root: shoot ratio (−10.7%) [54]. The preferential allocation to the canopy led to stronger water loss demands and a weaker water absorption from the soil [54,55]. Furthermore, the whole-tree water transport capacity would be weakened, as shown in our study (Figures 3 and 4). However, the depression effects under a high fertilization were not significant for *C. chinensis* (Figures 3 and 4). Xylem anatomic differences between the two species could matter since the highly efficient ring-porous conduits would provide more water for transpiration under a high fertilization [49]. However, more studies are needed to validate this assumption.

5. Conclusions

In this study, the water transport capacity was investigated on the whole-tree level under an enhanced N input for two dominated species, *S. superba* and *C. chinensis*. The J_S in this study was decoupled to that of the leaf transpiration reported in our previous study for both species (Zhang et al., 2021a). The enhanced isohydric behavior should be accountable, with an aim to maintain the stable leaf water potential. It is noted that the *S. superba* tended to behave more isohydrically than *C. chinensis*, which means that it might have benefited from its smaller conduits. In addition, the nitrogen effects displayed above were weakened under a high fertilization dose, which might be attributed to the stomatal closure or the prone of carbon allocation to the leaf instead of to the root. These results proved that the scale effects should be considered in the future work on the nitrogen additions effects.

Supplementary Materials: The following supporting information can be downloaded at: https://www.mdpi.com/article/10.3390/f13111847/s1, Figure S1: Schematic representation of assessing changes in sensitivity changes about the G_S to VPD. J_S decreases with increasing VPD (**A**). We extracted the upper threshold values of J_S and VPD and fitted a straight line, the slope of the straight line was then found for ANOVA to analyze the change in the sensitivity of G_S to VPD (**B**); Figure S2: There is no significant difference in leaf area index(LAI), tree height(H) and the stem diameter at breast height (DBH) for both species before and after our experiment lasting for one year. Before the analysis, a homogeneity test of variance was conducted to test the data homogeneity. The analyses of variance (ANOVA) were constructed with SPSS 18 (IBM Inc., USA) to test the fixed effects of N addition, the species and their interactions (N treatments × species) for the three variables.

Author Contributions: Z.Z. (Zhenzhen Zhang) and P.Z. conceived the study; Z.Z. (Zhen Zhao) and Z.Z. (Zhenzhen Zhang) designed and carried out the analyses. L.O., X.Z., L.Z. (Liwei Zhu), C.C. and L.Z. (Linhui Zeng) conducted the experiments, and Z.Z. (Zhen Zhao) wrote the manuscript. All authors critically contributed to the drafts and gave final approval for publication. All authors have read and agreed to the published version of the manuscript.

Funding: This research was funded by National Natural Science Foundation of China grant number 41701226 and U21A2003, Zhejiang Province Public Welfare Technology Application Research Project grant number LGF19C030002, and Zhejiang Normal University Key Laboratory of Watershed Earth Surface Processes and Ecological Security Research Project grant number KF-2022-21.

Data Availability Statement: The datasets for this study can be found in the dryad digital repository at https://doi.org/10.5061/dryad.rbnzs7hf6 (accessed on 25 October 2022).

Conflicts of Interest: The authors declare that the research was conducted in the absence of any commercial or financial relationships that could be construed as a potential conflict of interest.

References

1. Fang, Y.; Yoh, M.; Koba, K.; Zhu, W.; Takebayashi, Y.; Xiao, Y.; Lei, C.; Mo, J.; Zhang, W.; Lu, X. Nitrogen deposition and forest nitrogen cycling along an urban-rural transect in southern China. *Glob. Chang. Biol.* **2011**, *17*, 872–885. [CrossRef]
2. Jia, Y.; Yu, G.; He, N.; Zhan, X.; Fang, H.; Sheng, W.; Zuo, Y.; Zhang, D.; Wang, Q. Spatial and decadal variations in inorganic nitrogen wet deposition in China induced by human activity. *Sci. Rep.* **2014**, *4*, 3763. [CrossRef] [PubMed]
3. Mao, J.; Mao, Q.; Gundersen, P.; Gurmesa, G.A.; Zhang, W.; Huang, J.; Wang, S.; Li, A.; Wang, Y.; Guo, Y.; et al. Unexpected high retention of ^{15}N-labeled nitrogen in a tropical legume forest under long-term nitrogen enrichment. *Glob. Chang. Biol.* **2021**, *28*, 1529–1543. [CrossRef] [PubMed]
4. Xing, A.; Du, E.; Shen, H.; Xu, L.; de Vries, W.; Zhao, M.; Liu, X.; Fang, J. Nonlinear responses of ecosystem carbon fluxes to nitrogen deposition in an old-growth boreal forest. *Ecol. Lett.* **2022**, *25*, 77–88. [CrossRef]
5. Hacke, U.G.; Plavcová, L.; Almeida-Rodriguez, A.; King-Jones, S.; Zhou, W.; Cooke, J.E. Influence of nitrogen fertilization on xylem traits and aquaporin expression in stems of hybrid poplar. *Tree Physiol.* **2010**, *30*, 1016–1025. [CrossRef]
6. Chiwa, M. Long-term changes in atmospheric nitrogen deposition and stream water nitrate leaching from forested watersheds in western Japan. *Environ. Pollut.* **2021**, *287*, 117634. [CrossRef]
7. Lu, X.; Vitousek, P.M.; Mao, Q.; Gilliam, F.S.; Luo, Y.; Turner, B.L.; Zhou, G.; Mo, J. Nitrogen deposition accelerates soil carbon sequestration in tropical forests. *Proc. Natl. Acad. Sci. USA* **2021**, *118*, e2020790118. [CrossRef]
8. Adams, M.A.; Buckley, T.N.; Binkley, D.; Neumann, M.; Turnbull, T.L. CO_2, nitrogen deposition and a discontinuous climate response drive water use efficiency in global forests. *Nat. Commun.* **2021**, *12*, 5194. [CrossRef]
9. Jin, Y.; Wang, C.; Zhou, Z.; Gu, J. Contrasting responses of hydraulic traits between leaf and branch to 16-year nitrogen addition in a larch plantation. *For. Ecol. Manag.* **2020**, *475*, 118461. [CrossRef]
10. Liang, X.; Zhang, T.; Lu, X.; Ellsworth, D.S.; BassiriRad, H.; You, C.; Wang, D.; He, P.; Deng, Q.; Liu, H.; et al. Global response patterns of plant photosynthesis to nitrogen addition: A meta-analysis. *Glob. Chang. Biol.* **2020**, *26*, 3585–3600. [CrossRef]
11. Forrester, D.I.; Collopy, J.J.; Beadle, C.L.; Warren, C.R.; Baker, T.G. Effect of thinning, pruning and nitrogen fertiliser application on transpiration, photosynthesis and water-use efficiency in a young *Eucalyptus nitens* plantation. *For. Ecol. Manag.* **2012**, *266*, 286–300. [CrossRef]
12. Matimati, I.; Verboom, G.A.; Cramer, M.D. Nitrogen regulation of transpiration controls mass-flow acquisition of nutrients. *J. Exp. Bot.* **2014**, *65*, 159–168. [CrossRef] [PubMed]
13. Zhang, T.; Liang, X.; Ye, Q.; BassiriRad, H.; Liu, H.; He, P.; Wu, G.; Lu, X.; Mo, J.; Cai, X.; et al. Leaf hydraulic acclimation to nitrogen addition of two dominant tree species in a subtropical forest. *Sci. Total Environ.* **2021**, *771*, 145415. [CrossRef]
14. Zhang, Z.; Zhao, P.; Ouyang, L.; Zhao, X.; Zhu, L.; Ni, G. Divergent Responses of Dominant Forest Tree Species to Manipulated Canopy and Understory N Additions in Terms of Foliage Stoichiometric, Photosynthetic, and Hydraulic Traits. *J. Geophys. Res. Biogeosciences* **2021**, *126*, e2021JG006579. [CrossRef]
15. Hu, Y.; Zhao, P.; Zhu, L.; Zhao, X.; Ni, G.; Ouyang, L.; Schäfer, K.V.; Shen, W. Responses of sap flux and intrinsic water use efficiency to canopy and understory nitrogen addition in a temperate broadleaved deciduous forest. *Sci. Total Environ.* **2019**, *648*, 325–336. [CrossRef]
16. Ouyang, L.; Zhao, P.; Zhu, L.; Zhang, Z.; Zhao, X.; Ni, G. Difference in response of water use to evaporative demand for codominant diffuse-porous versus ring-porous tree species under N addition in a temperate forest. *Ecohydrology* **2017**, *10*, e1829. [CrossRef]
17. Wang, Q.; Lintunen, A.; Zhao, P.; Shen, W.; Salmon, Y.; Chen, X.; Ouyang, L.; Zhu, L.; Ni, G.; Sun, D.; et al. Assessing Environmental Control of Sap Flux of Three Tree Species Plantations in Degraded Hilly Lands in South China. *Forests* **2020**, *11*, 206. [CrossRef]

18. Zhang, Z.; Zhou, J.; Zhao, P.; Zhao, X.; Zhu, L.; Ouyang, L.; Ni, G. Validation and in situ application of a modified thermal dissipation probe for evaluating standing water use of a clumped bamboo: *Bambusa chungii*. *Agric. For. Meteorol.* **2017**, *239*, 15–23. [CrossRef]
19. Addington, R.N.; Mitchell, R.J.; Oren, R.; Donovan, L. Stomatal sensitivity to vapor pressure deficit and its relationship to hydraulic conductance in Pinus palustris. *Tree Physiol.* **2004**, *24*, 561–569. [CrossRef]
20. Klein, T. The variability of stomatal sensitivity to leaf water potential across tree species indicates a continuum between isohydric and anisohydric behaviours. *Funct. Ecol.* **2014**, *28*, 1313–1320. [CrossRef]
21. Gleason, S.M.; Wiggans, D.R.; Bliss, C.A.; Comas, L.H.; Cooper, M.; DeJonge, K.C.; Young, J.S.; Zhang, H. Coordinated decline in photosynthesis and hydraulic conductance during drought stress in *Zea mays*. *Flora* **2017**, *227*, 1–9. [CrossRef]
22. Rodríguez-Gamir, J.; Primo-Millo, E.; Forner-Giner, M. An Integrated View of Whole-Tree Hydraulic Architecture. Does Stomatal or Hydraulic Conductance Determine Whole Tree Transpiration? *PLoS ONE* **2016**, *11*, e0155246. [CrossRef] [PubMed]
23. Lauriks, F.; Salomón, R.L.; De Roo, L.; Goossens, W.; Leroux, O.; Steppe, K. Limited plasticity of anatomical and hydraulic traits in aspen trees under elevated CO_2 and seasonal drought. *Plant Physiol.* **2021**, *188*, 268–284. [CrossRef]
24. Macieira, B.P.B.; Locosselli, G.M.; Buckeridge, M.S.; Jardim, V.C.; Krottenthaler, S.; Anhuf, D.; Helle, G.; Cuzzuol, G.R.F.; Ceccantini, G. Will climate change shift carbon allocation and stem hydraulics? Insights on a systemic view of carbon- and water-related wood traits in an anysohydric tropical tree species (*Hymenaea courbaril*, Leguminosae). *Ecol. Indic.* **2021**, *128*, 107798. [CrossRef]
25. Bryant, K.N.; Fredericksen, B.W.; Rosenthal, D.M. Ring- and diffuse-porous species exhibit a spectrum of hydraulic behaviors from isohydry to anisohydry in a temperate deciduous forest. *Trees* **2021**, *36*, 485–495. [CrossRef]
26. Conesa, M.; de la Rosa, J.; Domingo, R.; Bañon, S.; Pérez-Pastor, A. Changes induced by water stress on water relations, stomatal behaviour and morphology of table grapes (cv. *Crimson Seedless*) grown in pots. *Sci. Hortic.* **2016**, *202*, 9–16. [CrossRef]
27. Lovisolo, C.; Perrone, I.; Carra, A.; Ferrandino, A.; Flexas, J.; Medrano, H.; Schubert, A. Drought-induced changes in development and function of grapevine (*Vitis* spp.) organs and in their hydraulic and non-hydraulic interactions at the whole-plant level: A physiological and molecular update. *Funct. Plant Biol.* **2010**, *37*, 98–116. [CrossRef]
28. Rogiers, S.Y.; Greer, D.H.; Hatfield, J.M.; Hutton, R.J.; Clarke, S.J.; Hutchinson, P.A.; Somers, A. Stomatal response of an anisohydric grapevine cultivar to evaporative demand, available soil moisture and abscisic acid. *Tree Physiol.* **2012**, *32*, 249–261. [CrossRef]
29. Zhang, Y.; Oren, R.; Kang, S. Spatiotemporal variation of crown-scale stomatal conductance in an arid *Vitis vinifera* L. cv. Merlot vineyard: Direct effects of hydraulic properties and indirect effects of canopy leaf area. *Tree Physiol.* **2012**, *32*, 262–279. [CrossRef]
30. Huang, J.-G.; Guo, X.; Rossi, S.; Zhai, L.; Yu, B.; Zhang, S.; Zhang, M. Intra-annual wood formation of subtropical Chinese red pine shows better growth in dry season than wet season. *Tree Physiol.* **2018**, *38*, 1225–1236. [CrossRef]
31. Zhen-Zhen, Z.; Ping, Z.; Jin-Xiu, Z.; Yao, S. Conduits anatomical structure and leaf traits of diffuse- and ring-porous stems in subtropical evergreen broad-leaved forests. *Chin. J. Plant Ecol.* **2019**, *43*, 131–138. [CrossRef]
32. Du, E.; Jiang, Y.; Fang, J.; de Vries, W. Inorganic nitrogen deposition in China's forests: Status and characteristics. *Atmos. Environ.* **2014**, *98*, 474–482. [CrossRef]
33. Deutsch, C.; Weber, T. Nutrient Ratios as a Tracer and Driver of Ocean Biogeochemistry. *Annu. Rev. Mar. Sci.* **2012**, *4*, 113–141. [CrossRef] [PubMed]
34. Zhang, W.; Shen, W.; Zhu, S.; Wan, S.; Luo, Y.; Yan, J.; Wang, K.; Liu, L.; Dai, H.; Li, P.; et al. CAN Canopy Addition of Nitrogen Better Illustrate the Effect of Atmospheric Nitrogen Deposition on Forest Ecosystem? *Sci. Rep.* **2015**, *5*, 11245. [CrossRef]
35. Granier, A. Evaluation of transpiration in a Douglas-fir stand by means of sap flow measurements. *Tree Physiol.* **1987**, *3*, 309–320. [CrossRef]
36. Köstner, B.M.M.; Schulze, E.D.; Kelliher, F.M.; Hollinger, D.Y.; Byers, J.N.; Hunt, J.; McSeveny, T.M.; Meserth, R.; Weir, P.L. Transpiration and canopy conductance in a pristine broad-leaved forest of Nothofagus: An analysis of xylem sap flow and eddy correlation measurements. *Oecologia* **1992**, *91*, 350–359. [CrossRef]
37. Campbell, G.S.; Norman, J.M. The Light Environment of Plant Canopies. In *An Introduction to Environmental Biophysics*; Springer: New York, NY, USA, 1998; pp. 247–278. [CrossRef]
38. Zhang, Z.; Zhao, P.; Zhao, X.; Zhou, J.; Zhao, P.; Zeng, X.; Hu, Y.; Ouyang, L. The tree height-related spatial variances of tree sap flux density and its scale-up to stand transpiration in a subtropical evergreen broadleaf forest. *Ecohydrology* **2018**, *11*, e1979. [CrossRef]
39. Zhang, Z.Z.; Zhao, P.; McCarthy, H.R.; Zhao, X.H.; Niu, J.F.; Zhu, L.W.; Ni, G.Y.; Ouyang, L.; Huang, Y.Q. Influence of the decoupling degree on the estimation of canopy stomatal conductance for two broadleaf tree species. *Agric. For. Meteorol.* **2016**, *221*, 230–241. [CrossRef]
40. Zhang, Z.; Zhao, P.; McCarthy, H.R.; Ouyang, L.; Niu, J.; Zhu, L.; Ni, G.; Huang, Y. Hydraulic Balance of a *Eucalyptus urophylla* Plantation in Response to Periodic Drought in Low Subtropical China. *Front. Plant Sci.* **2016**, *7*, 1346. [CrossRef]
41. Jiang, X.; Liu, N.; Lu, X.; Huang, J.-G.; Cheng, J.; Guo, X.; Wu, S. Canopy and understory nitrogen addition increase the xylem tracheid size of dominant broadleaf species in a subtropical forest of China. *Sci. Total Environ.* **2018**, *642*, 733–741. [CrossRef]
42. Clearwater, M.; Meinzer, F. Relationships between hydraulic architecture and leaf photosynthetic capacity in nitrogen-fertilized *Eucalyptus grandis* trees. *Tree Physiol.* **2001**, *21*, 683–690. [CrossRef]

43. Dao, M.C.E.; Rossi, S.; Walsh, D.; Morin, H.; Houle, D. A 6-Year-Long Manipulation with Soil Warming and Canopy Nitrogen Additions does not Affect Xylem Phenology and Cell Production of Mature Black Spruce. *Front. Plant Sci.* **2015**, *6*, 877. [CrossRef] [PubMed]
44. Collins, M.J.; Fuentes, S.; Barlow, E.W.R. Partial rootzone drying and deficit irrigation increase stomatal sensitivity to vapour pressure deficit in anisohydric grapevines. *Funct. Plant Biol.* **2010**, *37*, 128–138. [CrossRef]
45. Zhang, Z.-Z.; Yang, K.-J.; Gu, Y.-L.; Zhao, P.; Ouyang, L. Effects of simulated changes in precipitation pattern on sap flux in two tree species in subtropical region. *Chin. J. Plant Ecol.* **2019**, *43*, 988–998. [CrossRef]
46. Gao, J.; Zhao, P.; Shen, W.; Niu, J.; Zhu, L.; Ni, G. Biophysical limits to responses of water flux to vapor pressure deficit in seven tree species with contrasting land use regimes. *Agric. For. Meteorol.* **2015**, *200*, 258–269. [CrossRef]
47. Leigang, S.; Shaoqiang, W.; Mickler, R.A.; Jinghua, C.; Quanzhou, Y.; Zhaohui, Q.; Guoyi, Z.; Ze, M. Remote Sensing Indices to Measure the Seasonal Dynamics of Photosynthesis in a Southern China Subtropical Evergreen Forest. *J. Resour. Ecol.* **2019**, *10*, 112–126. [CrossRef]
48. Domec, J.-C.; Johnson, D.M. Does homeostasis or disturbance of homeostasis in minimum leaf water potential explain the isohydric versus anisohydric behavior of *Vitis vinifera* L. cultivars? *Tree Physiol.* **2012**, *32*, 245–248. [CrossRef]
49. McCulloh, K.; Sperry, J.S.; Lachenbruch, B.; Meinzer, F.; Reich, P.; Voelker, S. Moving water well: Comparing hydraulic efficiency in twigs and trunks of coniferous, ring-porous, and diffuse-porous saplings from temperate and tropical forests. *New Phytol.* **2010**, *186*, 439–450. [CrossRef]
50. Manzoni, S.; Vico, G.; Thompson, S.; Beyer, F.; Weih, M. Contrasting leaf phenological strategies optimize carbon gain under droughts of different duration. *Adv. Water Resour.* **2015**, *84*, 37–51. [CrossRef]
51. Omondi, J.O.; Lazarovitch, N.; Rachmilevitch, S.; Yermiyahu, U.; Sperling, O. High Nitrogen Availability Limits Photosynthesis and Compromises Carbohydrate Allocation to Storage in Roots of *Manihot esculenta* Crantz. *Front. Plant Sci.* **2019**, *10*, 1041. [CrossRef]
52. Bauer, G.A.; Berntson, G.M.; Bazzaz, F.A. Regenerating temperate forests under elevated CO_2 and nitrogen deposition: Comparing biochemical and stomatal limitation of photosynthesis. *New Phytol.* **2001**, *152*, 249–266. [CrossRef]
53. Daley, M.J.; Phillips, N.G. Interspecific variation in nighttime transpiration and stomatal conductance in a mixed New England deciduous forest. *Tree Physiol.* **2006**, *26*, 411–419. [CrossRef] [PubMed]
54. Li, W.; Jin, C.; Guan, D.; Wang, Q.; Wang, A.; Yuan, F.; Wu, J. The effects of simulated nitrogen deposition on plant root traits: A meta-analysis. *Soil Biol. Biochem.* **2015**, *82*, 112–118. [CrossRef]
55. Smithwick, E.A.H.; Eissenstat, D.M.; Lovett, G.M.; Bowden, R.D.; Rustad, L.E.; Driscoll, C.T. Root stress and nitrogen deposition: Consequences and research priorities. *New Phytol.* **2013**, *197*, 712–719. [CrossRef] [PubMed]
56. Wang, G.; Liu, F. Carbon allocation of Chinese pine seedlings along a nitrogen addition gradient. *For. Ecol. Manag.* **2014**, *334*, 114–121. [CrossRef]